Articles

Gel Phase Polymorphism in Ether-Linked Dihexadecylphosphatidylcholine Bilayers†

J. T. Kim, J. Mattai, and G. G. Shipley*

Biophysics Institute, Housman Medical Research Center, Departments of Medicine and Biochemistry, Boston University School of Medicine, Boston, Massachusetts 02118

Received February 20, 1987; Revised Manuscript Received May 12, 1987

ABSTRACT: The structure and properties of the ether-linked 1,2-dihexadecylphosphatidylcholine (DHPC) have been examined as a function of hydration. By differential scanning calorimetry, DHPC exhibits an endothermic (chain melting) transition with the transition temperature (limiting value, 44.2 °C) and enthalpy (limiting value, ΔH = 8.0 kcal/mol) being hydration dependent. For hydration values >30 wt % water, DHPC exhibits a pretransition at ~36 °C (ΔH = 1.1 kcal/mol) and a subtransition at ~5 °C (ΔH = 0.2 kcal/mol). By X-ray diffraction, at 22 °C DHPC exhibits a normal bilayer gel structure with the bilayer periodicity increasing from 58.0 to 62.5 Å over the hydration range 9.5–25.4% water. At 30–32% water, two coexisting gel phases are observed with d = 63–64 Å and d = 44–45 Å; at higher hydration, only the latter phase is present, reaching a limiting d = 47.0 Å at 37.5% water. Two different gel phases clearly exist at low and high hydrations. Electron density profiles at low hydration (9.5–25.4%) show a bilayer thickness d_{p-p} = 46 Å, whereas at >32% water the bilayer thickness is markedly reduced, d_{p-p} = 30 Å. These and other structural parameters indicate a hydration-dependent gel → gel structural transition between a normal bilayer (two chains per polar group) and the chain-interdigitated bilayer (four chains per polar group) arrangement described previously for DHPC [Ruocco, M. J., Siminovitch, D. J., & Griffin, R. G. (1985) *Biochemistry 24*, 2406–2411]. In contrast, at 65 °C the normal liquid-crystalline bilayer structure (d = 51.0–60.0 Å; d_{p-p} = 38 Å) is present at all hydrations. Comparisons of the hydration-dependent structural behavior of DHPC are made with its ester analogue 1,2-dipalmitoylphosphatidylcholine.

In addition to the diacylphospholipids, significant amounts of alkyl–acyl- or dialkylphospholipids are found in plasma and organelle membranes [for reviews, see Mangold and Paltauf (1981) and Horrocks and Sharma (1982)]. For example, myelin membrane is enriched in plasmalogen phosphatidylethanolamine with a 1-alk-1-enyl-2-acyl chain linkage to the glycerol moiety [see Horrocks and Sharma (1982)]. An exciting discovery in the lipid field is that the platelet activating factor eliciting a variety of important biological responses is 1-alkyl-2-acetylphosphatidylcholine [for a review, see Snyder et al. (1985)]. Heart tissue is unique in that it contains significant amounts of choline plasmalogen as well as smaller quantities of dialkylphosphatidylcholines [see Horrocks and Sharma (1982)], but as yet no well-defined role for these lipids has been elucidated. Halophilic bacteria, including *Halobacterium halobium* and *Halobacterium cutirubrum*, are rich in dialkylglycerolipids such as the diphytanyl ether analogue of phosphatidylglycerophosphate (Kates, 1978). Finally, in anaerobic bacteria such as *Clostridium butyricum*, ethanolamine plasmalogens are prevalent, and the regulatory functions of these lipids are currently being investigated (Goldfine, 1985; Goldfine et al., 1987).

In contrast to diacylphospholipids, relatively few studies of the properties of alkyl–acyl or dialkylphospholipids have been reported. For dialkyllipids, some comparisons can be made with the corresponding diacyllipids. For example, dihexadexylphosphatidylethanolamine (DHPE) exhibits a higher chain melting transition but a lower bilayer → hexagonal transition than the corresponding diacyllipid, dipalmitoyl-PE (Vaughan & Keough, 1974; Boggs et al., 1981; Seddon et al., 1983). It is thought that these changes arise from alterations in both the chain packing and the intermolecular hydrogen-bonding arrangement [see Hitchock et al. (1974)] as a consequence of the ether vs. ester chain linkage (Boggs et al., 1981; Seddon et al., 1983). Comparisons have also been made between dihexadecylphosphatidylcholine (DHPC) and dipalmitoyl-PC (DPPC). The ether-linked DHPC exhibits a slightly higher transition temperature (44–45 °C) than the corresponding ester analogue DPPC (41.5 °C), but in general, the two PCs exhibit similar thermotropic behavior (Vaughan & Keough, 1974; Ruocco et al., 1985a). Other physical studies also suggest strong similarities. For example, DHPC and DPPC exhibit similar surface monolayer behavior, indicating similar packing arrangements in either their liquid-expanded or their condensed monolayer states, although differences in surface potential are observed (Paltauf et al., 1971). ^{31}P, ^{2}H, and ^{14}N NMR studies of DHPC, DPPC, and short-chain analogues (Ruocco et al., 1985a,b; Hauser, 1981; Hauser et al., 1981) suggest similar average conformations and segmental motions of the phosphorylcholine polar group of both ether- and ester-linked PCs in gel, liquid-crystalline, monomeric, and micellar states.

However, in spite of the overall similarity of DHPC and DPPC, there are some notable differences. ^{14}N quadrupolar splittings of DHPC in the liquid-crystalline phase are greater (indicative of a decrease in orientational order around the C–N bond of the polar group) than those of DPPC (Siminovitch et al., 1983). ^{2}H NMR studies of DHPC deuterium labeled at the α-position of the two alkyl chains show a more complex pattern of quadrupolar splittings than that of "similarly" labeled DPPC, again indicative of conformational differences

† This research was supported by Research Grant HL-26335 and Training Grant HL-07291 from the National Institutes of Health.

0006-2960/87/0426-6592$01.50/0

in the "interfacial" region, at least when DHPC and DPPC are present in the liquid-crystalline phase (Ruocco et al., 1985b). Perhaps the most surprising difference between DHPC and DPPC lies in the structure of their respective gel phases. Ruocco et al. (1985a) have shown that fully hydrated DHPC exhibits subtransitions, pretransitions, and chain melting transitions similar to but not identical with those exhibited by DPPC. Further, they show that the diffraction patterns of the subgel and gel phases of DHPC and DPPC differ markedly. Notably, the bilayer periodicities and the derived electron density profiles indicate significantly smaller bilayer thicknesses (~30 Å) for DHPC gel phases than the corresponding phases of DPPC (bilayer thickness ~44 Å). This suggests that for DHPC the bilayers are fully chain interdigitated (Ruocco et al., 1985a). A number of phospholipids capable of forming chain-interdigitated phases either by spontaneous means or by induction have been reported recently (Ranck et al., 1977; Serrallach et al., 1983; McDaniel et al., 1983; McIntosh et al., 1983; Braganza & Worcester, 1986). Thus, what appear to be relatively minor changes in the interfacial region can result in significant structural differences between DHPC and DPPC. In this study, we focus on the hydration dependence of the gel phase structure of DHPC, and in the following paper (Kim et al., 1987), we describe the gel phase miscibility of DHPC and DPPC.

Materials and Methods

DHPC was obtained from Berchtold (Berne, Switzerland) and purified by column chromatography using Iatrobeads 8060 (Iatron Laboratories, Tokyo, Japan). The DHPC was shown to be >99% pure by thin-layer chromatography using the solvent system chloroform/methanol/water (65:25:4 v/v).

For differential scanning calorimetry (DSC), samples of anhydrous DHPC were weighed into stainless steel pans, appropriate amounts of distilled, deionized water were added gravimetrically, and the pans were hermetically sealed. Scanning calorimetry was performed on a Perkin-Elmer DSC-2 calorimeter over the temperature range −8 to 87 °C. Samples were heated and cooled at least 4 times to achieve equilibration. The transition temperatures were determined from the peaks of the observed transitions, and the transition enthalpies were determined from the areas under the curves as measured with a planimeter and calibrated by using a known standard (gallium). For fully hydrated samples, additional DSC experiments were performed with a Microcal (Amherst, MA) 2 calorimeter. DHPC (0.04 wt %) dispersions were examined at a heating rate of 45 °C/h.

For X-ray diffraction, hydrated samples were prepared by weighing DHPC into thin-walled glass capillaries followed by the addition of distilled, deionized water. The capillaries were flame-sealed and coated at the seal with epoxy glue to eliminate leaks. Homogeneous mixing of the samples was achieved by cycles of centrifugation, sample inversion, and recentrifugation at a temperature greater than the (chain melting) transition temperature. X-ray diffraction patterns were recorded on photographic film using nickel-filtered Cu Kα radiation (λ = 1.5418 Å) from an Elliott GX-6 rotating anode generator (Elliott Automation, Borehamwood, U.K.). The X-ray beam was focused by using either double-mirror (Franks, 1958) or toroidal (Elliott, 1965) optics. Microdensitometry was performed with a Joyce Loebl Model III-CS scanning microdensitometer.

Results

Scanning Calorimetry of Hydrated DHPC. DSC heating curves of DHPC at different hydrations (range 4.8–61.0 wt % water) are shown in Figure 1. Fully hydrated DHPC exhibits three different transitions: a low-temperature subgel transition, T_S, a pretransition, T_P, at intermediate temperatures, and a high-temperature (chain melting) transition, T_M (Figure 1). With increasing water content, the chain melting transition gradually decreases from 74.2 °C (note also the shoulder at 72.0 °C) at 4.8% water to a limiting value of 44.2 °C at >30% water (Figure 2A). In addition, the transition width decreases with increasing hydration (see Figure 1) whereas the transition enthalpy increased from 5.5 kcal/mol of DHPC, again reaching a limiting value (8.0 kcal/mol) at ~35% water (Figure 2B). For hydration levels >30% water, a pretransition is observed at ~36 °C (ΔH = 1.1 kcal/mol of DHPC), shown in Figures 1 and 2. Similarly the subgel transition at ~5 °C (ΔH = 0.2 kcal/mol of DHPC) is only observed at >30% hydration (see Figures 1 and 2). Transition entropies for T_S, T_P, and T_M are also plotted in Figure 2B. Identical calorimetric behavior is observed for fully hydrated DHPC recorded at a much slower heating rate (45 °C/h) on a high-sensitivity calorimeter (data not shown).

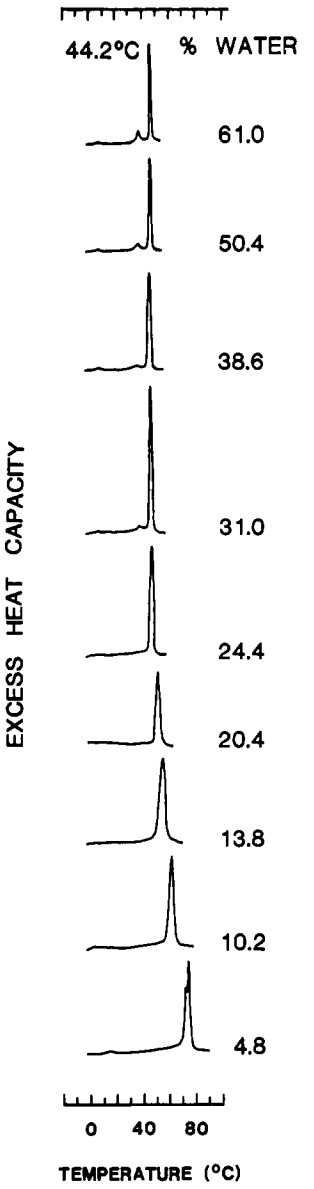

FIGURE 1: Representative DSC heating curves of hydrated DHPC in the range 4.8–61.0 wt % water. Heating rates: 5 °C/min.

X-ray Diffraction of Hydrated DHPC. X-ray diffraction patterns were recorded for hydrated DHPC at temperatures between the sub- and pretransitions (at 22 °C; gel phase) and

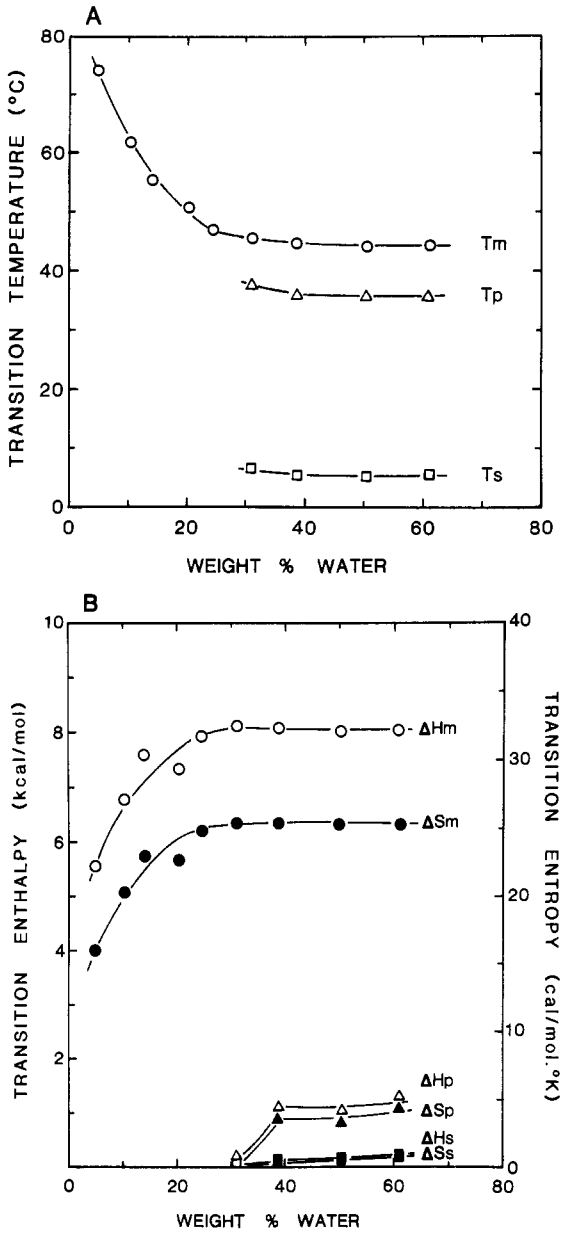

FIGURE 2: Transition temperatures (A), enthalpies (B), and entropies (B) of the subtransitions (squares), pretransitions (triangles), and chain melting transitions (circles) of DHPC as a function of hydration.

above the chain melting transition (at 65 °C; liquid-crystalline phase). Representative diffraction patterns for DHPC at 13.6% and 49.7% hydration are shown in Figure 3. At 22 °C, DHPC (13.6% water) shows eight lamellar reflections, indicative of bilayer geometry with d = 58.4 Å (Figure 3A). The wide-angle region shows a strong reflection at 1/4.28 Å^{-1} (arrowed) indicative of hexagonal chain packing. At higher hydration (49.7% water), DHPC exhibits five lamellar reflections corresponding to a markedly reduced bilayer periodicity d = 47.0 Å (Figure 3B), similar to that observed by Ruocco et al. (1985a). Again, a single wide-angle reflection is observed at 1/4.08 Å^{-1} (arrowed). At 65 °C, DHPC shows six lamellar reflections (d = 50.8 Å) at 13.6% water (Figure 3C) and four lamellar reflections (d = 60.0 Å) at 49.7% water (Figure 3D). At both hydration levels, a broad reflection at 1/4.5 Å^{-1} (arrowed) characteristic of the melted chain, liquid-crystalline bilayer phase is observed.

The variation in the bilayer periodicity, representing the DHPC bilayer thickness plus the intercalated water layer, is shown for the bilayer gel phase at 22 °C and the bilayer liquid-crystalline phase at 65 °C in panels A and B, respectively, of Figure 4. At 22 °C, DHPC exhibits a single bilayer gel phase over the hydration range 9.5–25.4% water, and the bilayer periodicity increases from 58.4 to 62.4 Å (Figure 4A). At 30–32% water, two bilayer phases coexist, one of bilayer periodicity d = 63–64 Å and the other with a reduced periodicity of 44–45 Å (not shown). At higher hydration (>32% water), only the bilayer phase of reduced periodicity is observed. This bilayer phase exhibits some further hydration, reaching a hydration limit at ~37.5% water, d_{max} = 47.0 Å. According to the formalism of Luzzati (1968) and with the assumption that the partial specific volume of DHPC at 22 °C is identical with that of DPPC [$\bar{v}$ = 0.937 mL/g; see Nagle and Wilkinson (1978)], the derived parameters d_l (lipid thickness), d_w (water layer thickness), and S (surface area occupied per DHPC molecule at the lipid–water interface) have been calculated.[1] As shown in Figure 4A, over the hydration range 9.5–25.4% water, d_l decreases from 52.5 to 45.8 Å, d_w increases from 6.0 to 16.6 Å, and S increases from 41.8 to 48.0 Å^2. Then, over the hydration range 35–40% water, d_l decreases slightly to 28.8 Å, d_w increases slightly to 18.3 Å, and S increases slightly to 76.2 Å^2. Note the marked decrease in d_l (48.5 to 28.5 Å) and increase in S (48.0 to 76.2 Å^2) that occur at ~30% water as the DHPC gel phase changes structure.

The intensities of the low-angle reflections were used to determine the changes in structure amplitudes over the hydration range 9.5–25.4% water. This swelling method provides the continuous transform (the amplitude curve of the bilayer profile) from which the phases of the structure amplitudes can be determined, and it has been applied extensively to PC bilayer systems [see, for example, Torbet and Wilkins (1976), Janiak et al. (1979), McDaniel et al. (1983), Mattai and Shipley (1986), and McIntosh and Simon (1986)]. The observed intensities were corrected for Lorentz and polarization factors [$I(h)*h^2$] and different lamellar sets normalized with respect to each other according to standard procedures (Worthington & Blaurock, 1969). The normalized amplitudes are plotted as a function of reciprocal space coordinate s (s = 2 sin θ/λ) as shown in Figure 5A. The nodes, i.e., the points at which a phase change probably occurs, are suggested by the amplitude data alone and are confirmed by application of the Shannon sampling theorem [Shannon, 1949; Sayre, 1952; see Moody (1963), King and Worthington (1971), Worthington et al. (1973), Torbet and Wilkins (1976), Franks (1976), McIntosh et al. (1983), McIntosh and Simon (1986), and Mattai et al. (1987) for details of the method as applied to lipid bilayer systems]. This indicates that phase changes occur at s = 0.006, 0.035, 0.052, 0.078, and 0.093 Å^{-1} and the phase sequence for h = 1–6 is –, –, +, –, +, – for all hydrations. Corresponding electron density profiles, $\rho(X)$, are shown in Figure 6A (bottom). At all hydrations, a well-defined trough is observed at X = 0 Å, corresponding to the bilayer center, whereas the two peaks at approximately ±23 Å define the location of the electron-rich phosphate groups and their separation across the bilayer (d_{p-p}) provides an ad-

[1] Although equating the $\bar{v}$ of DHPC phases with those of "similar" gel and liquid-crystalline phases of DPPC is clearly an assumption, two pieces of information lead us to believe that this assumption is, at least, reasonably justified. First, as shown in Figure 4, for all phases the bilayer thicknesses calculated according to the Luzzati method (with the assumed values of $\bar{v}$) agree well with those derived directly from the electron density profiles (independent of $\bar{v}$). Second, with the noninterdigitated gel phase of 22 °C (20.3 wt % water) as an example, significant variations in $\bar{v}$ (range 0.877–0.977 cm^3/g) lead to only small changes in d_l (47.9–49.2 Å) and S (42.9–47.4 Å^2).

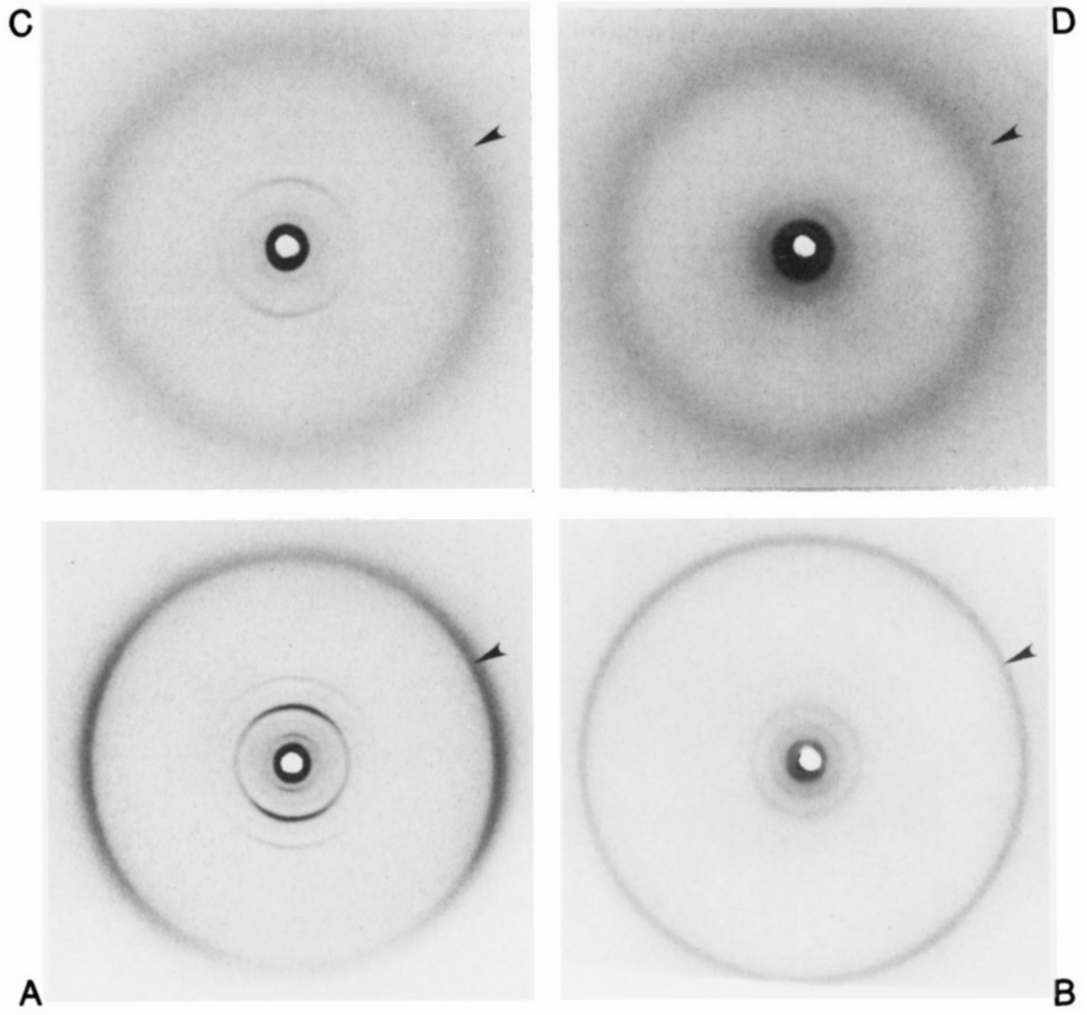

FIGURE 3: Representative X-ray diffraction patterns of hydrated DHPC. (A) 13.6% water; 22 °C. (B) 49.7% water; 22 °C. (C) 13.6% water; 65 °C. (D) 49.7% water; 65 °C. Note the orientation effects in the sample at low hydration (A and C).

ditional measure of the bilayer thickness. This approach suggests that the bilayer thickness is essentially independent of hydration with d_{p-p} constant at 46 Å (see also Figure 4A).

The phase of reduced periodicity present at water contents >30% exhibits minimal swelling (44–47 Å), and the above approach to phasing is not appropriate. Obviously, the normalized amplitudes do not fit on the amplitude curve of the bilayer phase present at low hydration (Figure 5A); however, by inspection, they are consistent with the amplitude curves from interdigitated gel phase bilayers studied previously [see McIntosh et al. (1983), McDaniel et al. (1983), and Mattai and Shipley (1986)]. In the hydration range 34.6–40.2% water, for h = 1–5 the phase sequence assigned is –, –, +, 0, –, and the corresponding calculated amplitude curve and electron density profiles are shown in Figures 5B and 6A (top). For these profiles, the central trough at X = 0 Å is less apparent, and the two peaks at $X = \pm 15$ Å indicate a reduced, but essentially constant, bilayer thickness, d_{p-p} = 30 Å (see also Figure 4A).

At 65 °C, a simpler pattern of behavior is observed (Figure 4B). DHPC exhibits a bilayer liquid-crystalline phase at all hydrations. The bilayer periodicity d increases from 51.0 Å at 13.6% water, reaching a limiting value d = 60.0 Å at ~35% water. d_l decreases and S increases with hydration, achieving limiting values [d_l = 39.0 Å; S = 61.0 Å^2, assuming $\bar{v}$ = 1.017 mL/g; see Nagle and Wilkinson (1978)] at ~25% water, whereas d_w continues to increase up to the hydration limit (i.e., ~35% water) with d_w(max) = 20 Å. The structure amplitude curve shows nodes at s = 0.006, 0.041, 0.061, and 0.087 Å^{-1} (Figure 5C). Over the hydration range 13.6–40.2% water, for h = 1–5 the phase sequence is –, –, +, –, + or –, –, +, –, –, depending on the hydration (see Figure 5C). The corresponding electron density profiles are shown in Figure 6B, and they resemble those of other liquid-crystalline PC bilayers. The bilayer thickness d_{p-p} is essentially independent of hydration over this range (d_{p-p} = 38 Å; see also Figure 4B).

Discussion

The structure and properties of the ester-linked DPPC have been studied exhaustively using a wide variety of physical methods. Hydrated DPPC exhibits a sequence of subtransitions, pretransitions, and chain melting transitions as DPPC converts between crystalline (L_c), gel ($L_{\beta'}$), rippled gel ($P_{\beta'}$), and liquid-crystalline (L_α) bilayer structures [for DSC and X-ray diffraction studies of DPPC, see, for example, Chapman et al. (1968), Tardieu et al. (1973), Janiak et al. (1976, 1979), Chen et al. (1980), Füldner (1981), and Ruocco and Shipley (1982a,b)]. The bilayer structures formed differ in terms of chain packing, chain tilt, etc., but for all gel phases at all hydrations studied, the two halves of the bilayer are relatively discrete, and extensive chain interdigitation across the bilayer center does not occur.

Recently, studies of DPPC analogues [e.g., 1,3-DPPC (Serrallach et al., 1983)] and DPPC in the presence of solvents other than water [e.g., ethanol (Simon & McIntosh, 1984), glycerol or ethylene glycol (McDaniel et al., 1983)] or surface

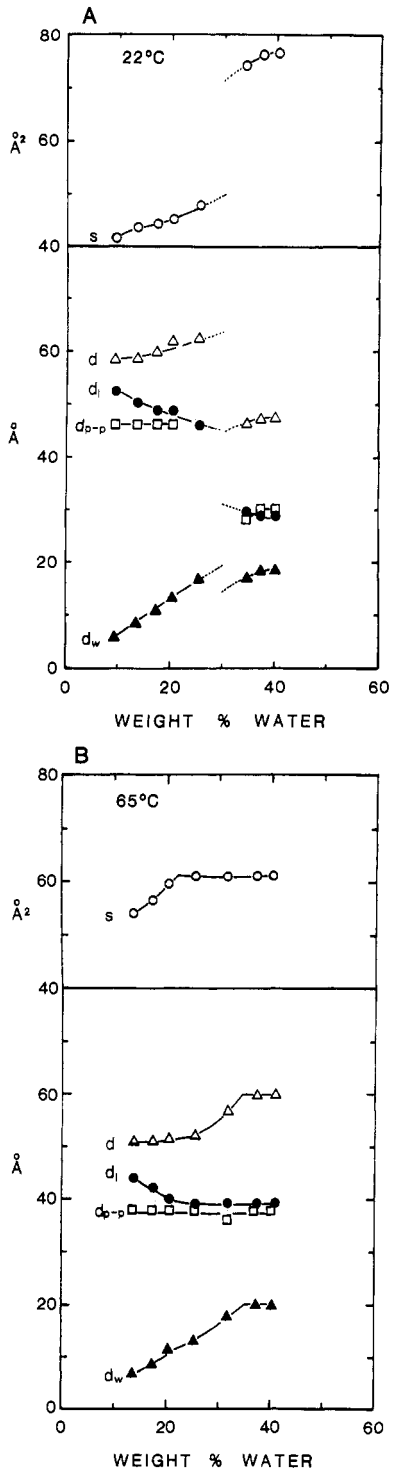

FIGURE 4: Bilayer structural parameters of DHPC as a function of water content at 22 °C (A) and 65 °C (B). (△) Bilayer periodicity, d (Å); (●) bilayer thickness, d_l (Å); (▲) water thickness, d_w (Å); (○) surface area per DHPC molecule at the lipid–water interface, S (Å^2); (□) phosphate–phosphate separation, d_{p-p} (Å), from electron density profiles (see Figure 6).

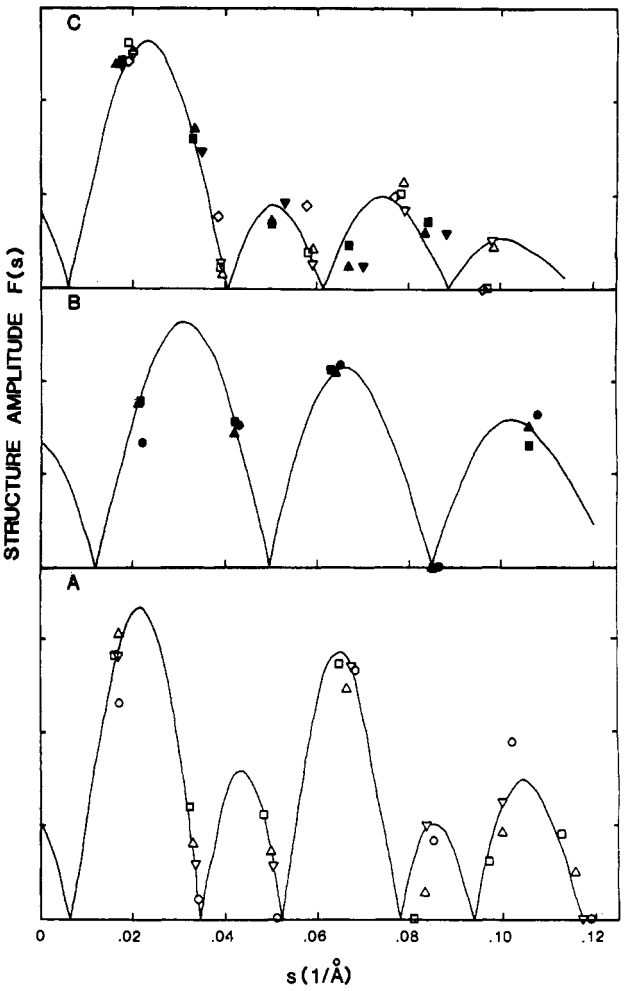

FIGURE 5: Structure amplitude of DHPC bilayers at 22 °C [low hydration (A) and high hydration (B)] and 65 °C (C). (A) (○) 9.5%; (▽) 13.6%; (△) 17.3%; (□) 20.3% water. (B) (●) 34.6%; (▲) 37.4%; (■) 40.2% water. (C) (▽) 13.6%; (△) 17.3%; (□) 20.3%; (◇) 25.4%; (▼) 31.6%; (▲) 37.4%; (■) 40.2%. The solid curves are calculated by using the Shannon sampling theory (see text): (A) 13.6% water; (B) 37.4% water; (C) 13.6% water.

active molecules [e.g., chlorpromazine (McIntosh et al., 1983)] have shown that alterations in the molecular geometry (1,3-DPPC) or "solvent" result in chain interdigitation in the gel phase, signaled by a marked reduction in the bilayer thickness. More recently, Braganza and Worcester (1986) have shown by neutron diffraction that the gel phase of DPPC is converted to an interdigitated bilayer gel phase at high pressures. Perhaps the most surprising observation is that of Ruocco et al. (1985a), who showed that DHPC at full hydration adopts exclusively chain-interdigitated gel and subgel phases. Thus, the relatively modest change in structure (ether vs. ester chain linkage) drastically influences the structure of the gel phases formed by DHPC and DPPC.

Here we have extended the studies of Ruocco et al. (1985a), focusing particularly on the hydration dependence of the structures of the gel and liquid-crystalline phases of DHPC. At low hydration (<30% water), DHPC exhibits a bilayer gel structure for which the bilayer parameters (d, d_l, S, d_{p-p}, and the electron density profiles; see Figures 4A and 6A) indicate the usual bilayer structure (i.e., noninterdigitated). In fact, over this hydration range (10–30% water), the structural parameters of DHPC are almost identical with those of DPPC (Ruocco & Shipley, 1982b), and a similar, perhaps tilted-chain, bilayer structure is indicated (see Figure 7). This bilayer structure is the stable phase below the chain melting transition, and no other gel phases are observed at <30% water. This bilayer phase undergoes a hydration-dependent chain-melting transition directly to the usual liquid-crystalline bilayer phase (see Figures 1, 2, and 7).

However, as the hydration is increased, at >30% water DHPC forms a different bilayer phase (see Figures 3B and 4A). This phase is characterized by marked changes in the bilayer parameters: d, d_l, and d_{p-p} all decrease by 15–18 Å, whereas S increases by ~30 Å^2 (see Figure 4A). In addition, the electron density profile (see Figure 6A) changes from that

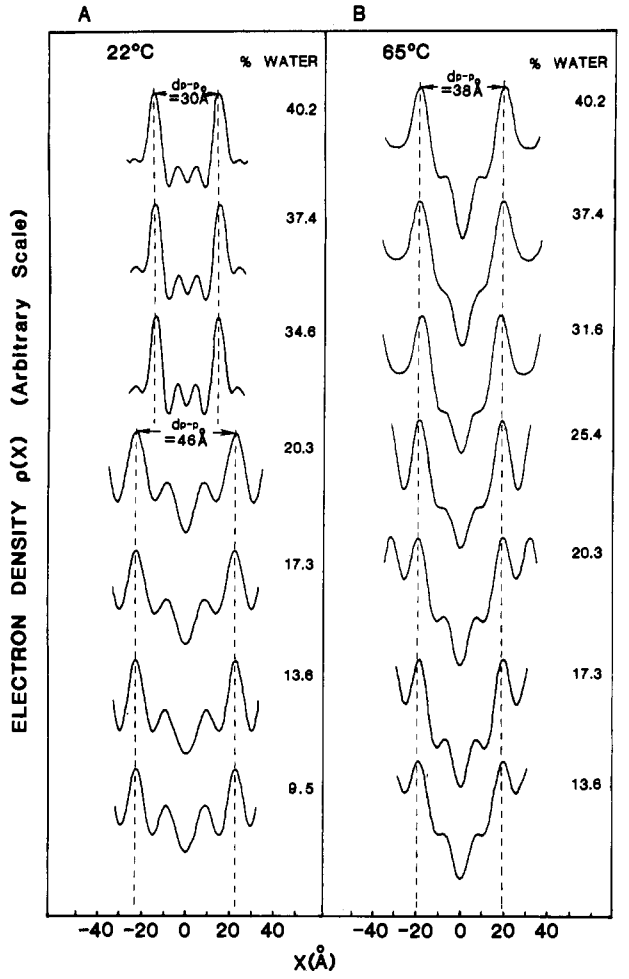

FIGURE 6: Electron density profiles, $\rho(X)$, of DHPC at different hydrations: (A) 22 °C and (B) 65 °C. Dashed lines: (A) ±23 Å (bottom), ±15 Å (top), (B) ±19 Å.

characteristic of a regular bilayer structure (well-defined trough at $X = 0$ Å) to that of an interdigitated bilayer (no well-defined trough at the bilayer center).

Thus, hydration alone promotes a gel → gel transition of DHPC in which the chains in apposing monolayers slide past each other to form the chain-interdigitated phase of reduced bilayer thickness and increased area per DHPC molecule (see Figure 7). Although the mechanism of this hydration-dependent gel → gel transition is unclear, presumably hydration effects at the polar group (e.g., altered polar group conformation, increased head-group area) trigger the bilayer conversion to the interdigitated chain packing arrangement. To improve on the structural description by Ruocco et al. (1985a), we had hoped to study the hydration dependence of the interdigitated phase but, as is clear from Figure 4A, at 22 °C its swelling range is limited to ~30–37.5% water. At 37.5% water, the DHPC phase is fully hydrated, and no further changes in structure occur at higher hydrations. The presence of a single, sharp wide-angle reflection at 1/4.08 Å^{-1} suggests that the chains are arranged perpendicular to the bilayer plane in this interdigitated phase of DHPC (shown schematically in Figure 7).

Additional changes in the properties of DHPC occur as the hydration exceeds 30% water. Notably, DHPC now exhibits the additional pre- and subtransitions previously described by Ruocco et al. (1985a). Thus, as with the pretransition of DPPC (Janiak et al., 1976), a certain hydration level is required for DHPC to exhibit the pre- and subtransitions. We note that the gel → gel transition occurs at the hydration at

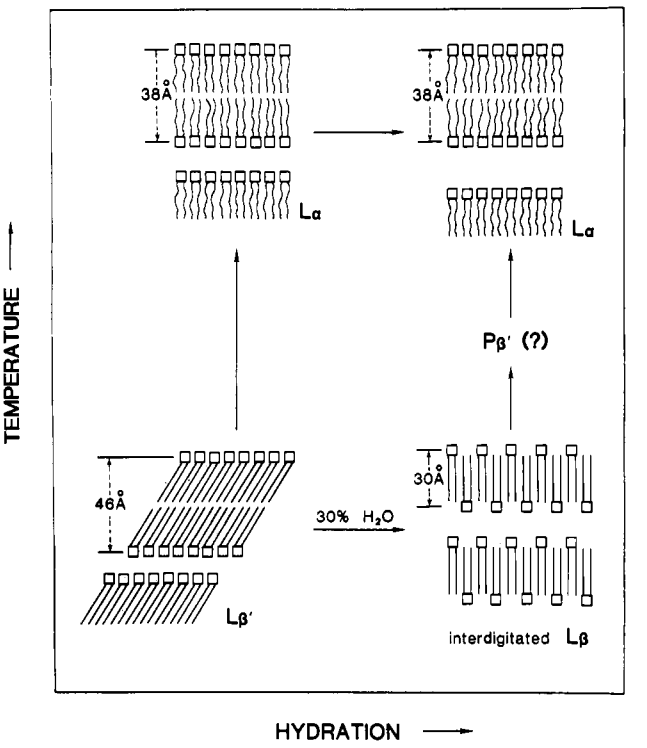

FIGURE 7: Structural representation of the hydration- and temperature-dependent transitions of DHPC. At low hydrations (<30% water), the reversible $L_{\beta'} \rightarrow L_\alpha$ transition is observed; at high hydrations (>30% water), the reversible $L_{\beta'} \rightarrow P_{\beta'} \rightarrow L_\alpha$ transitions are observed. At the bottom, the hydration-dependent noninterdigitated bilayer → interdigitated bilayer, gel → gel transition is emphasized.

which the chain melting transition has decreased to its limiting value (44.2 °C; see Figure 2A). Thus, at a point at which the increase in hydration apparently no longer changes the thermodynamic properties of hydrated DHPC (i.e., effective head-group hydration has been achieved), additional hydration induces the gel → gel transition. It is interesting that the hydration limit of the regular gel phase is identical with that of DPPC (30% water), corresponding to 19 water molecules per PC molecule [see Figure 4A and Ruocco and Shipley (1982b)]. For DPPC, this represents the absolute hydration limit, and no further change in structure is observed (Ruocco & Shipley, 1982b), whereas for DHPC additional hydration triggers the conversion to the interdigitated gel phase and allows the formation of additional gel (presumably $P_{\beta'}$) and subgel phases.[2] We note that the transition enthalpies and entropies of T_M and T_P of DHPC (see Figure 2B) are similar to those of the corresponding transitions of DPPC. In contrast, ΔH_S and ΔS_S are significantly lower than those of DPPC,

[2] Preliminary X-ray diffraction experiments have been performed at $T < T_S$ and $T_P < T < T_M$. Below T_S, DHPC exhibits a bilayer phase of periodicity $d = 47.4$ Å, suggesting that DHPC remains in a chain-interdigitated phase. Two diffraction lines at 4.23 and 3.82 Å are observed in the wide-angle region indicating changes in the lateral chain packing mode. Similar observations were reported previously by Ruocco et al. (1985a). Between T_P and T_M, DHPC gives a complex diffraction pattern in the low-angle region similar to but not identical with that exhibited by the two-dimensional, rippled $P_{\beta'}$ phase of DPPC [see Tardieu et al. (1973) and Janiak et al. (1976, 1979)]. Preliminary analyses suggest that the bilayer periodicity of DHPC increases markedly at T_P, indicating that both interdigitated → noninterdigitated chain packing changes and flat → rippled bilayer surface changes occur at T_P. Furthermore, the DHPC/DPPC phase diagram described in the following paper (Kim et al., 1987) indicates "solid solution" behavior between T_P and T_M. This, in turn, requires that the gel phase of DHPC be structurally related to that of DPPC which is known to be a noninterdigitated, rippled $P_{\beta'}$ phase.

suggesting that chain crystallization may not accompany the formation of the subgel phase of DHPC.

In contrast to these differences in structure and behavior of the gel phases of DHPC and DPPC, their structures above the chain melting transition appear identical. Their swelling curves appear superimposable, with identical hydration limits (35% water, 25 water molecules per PC molecule) and similar bilayer periodicities [see Figure 4B and Ruocco and Shipley (1982b)]. Thus, the conformational differences between DHPC and DPPC at the interfacial or polar group region responsible for the different gel phase behavior are no longer effective in the L_α phase following chain melting. In spite of recognizable conformational and dynamic differences between DHPC and DPPC revealed by NMR methods [see Siminovitch et al. (1983) and Ruocco et al. (1985b)], the bilayer structures formed and presumably the interbilayer forces are indistinguishable in the liquid-crystalline phases of DHPC and DPPC.

Finally, we have shown recently that fully hydrated mixtures of DHPC and DPPC can form both noninterdigitated and interdigitated gel bilayers depending on the DHPC:DPPC molar ratio (Kim et al., 1987). Interestingly, DHPC can be incorporated into a DPPC-rich noninterdigitated bilayer phase, and DPPC can be incorporated into a DHPC-rich interdigitated bilayer. Again, the structural "flexibility" of these PC molecules is apparent.

ACKNOWLEDGMENTS

We acknowledge useful discussions with Dr. M. J. Ruocco and Robert Nolte. We thank David Jackson for technical assistance and Irene Miller for help in preparing the manuscript.

Registry No. DHPC, 18545-87-4.

REFERENCES

Boggs, J. M., Stamp, D., Hughes, D. W., & Deber, C. M. (1981) *Biochemistry 20*, 5728–5735.

Braganza, L. F., & Worcester, D. L. (1986) *Biochemistry 25*, 2591–2596.

Chapman, D., Williams, R. M., & Ladbrooke, B. D. (1967) *Chem. Phys. Lipids 1*, 445–475.

Chen, S. C., Sturtevant, J. M., & Gaffney, B. J. (1980) *Proc. Natl. Acad. Sci. U.S.A. 77*, 5060–5063.

Elliott, A. J. (1965) *J. Sci. Instrum. 42*, 312–316.

Franks, A. (1958) *Br. J. Appl. Phys. 9*, 349–352.

Franks, N. P. (1976) *J. Mol. Biol. 100*, 345–358.

Füldner, H. H. (1981) *Biochemistry 20*, 5707–5710.

Goldfine, H. (1985) *Curr. Top. Cell. Regul. 26*, 163–174.

Goldfine, H., Johnston, N. C., Mattai, J., & Shipley, G. G. (1987) *Biochemistry 26*, 2814–2822.

Hauser, H. (1981) *Biochim. Biophys. Acta 646*, 203–210.

Hauser, H., Guyer, W., & Paltauf, F. (1981) *Chem. Phys. Lipids 29*, 103–120.

Hitchcock, P. B., Mason, R., Thomas, K. M., & Shipley, G. G. (1974) *Proc. Natl. Acad. Sci. U.S.A. 71*, 3036–3040.

Horrocks, L. A., & Sharma, M. (1982) in *Phospholipids* (Hawthorne, J. N., & Ansell, G. B., Eds.) pp 51–93, Elsevier, Amsterdam.

Janiak, M. J., Small, D. M., & Shipley, G. G. (1976) *Biochemistry 15*, 4575–4580.

Janiak, M. J., Small, D. M., & Shipley, G. G. (1979) *J. Biol. Chem. 254*, 6068–6078.

Kates, M. (1978) *Prog. Chem. Fats Other Lipids 15*, 301–342.

Kim, J. T., Mattai, J., & Shipley, G. G. (1987) *Biochemistry* (following paper in this issue).

King, G. I., & Worthington, C. R. (1971) *Phys. Lett. A 35*, 259–260.

Luzzati, V. (1968) in *Biological Membranes* (Chapman, D., Ed.) pp 71–123, Academic Press, London and New York.

Mangold, H. K., & Paltauf, F., Eds. (1981) *Ether Lipids: Biochemical and Biomedical Aspects*, Academic Press, New York.

Mattai, J., & Shipley, G. G. (1986) *Biochim. Biophys. Acta 859*, 257–265.

Mattai, J., Witzke, N. M., Bittman, R., & Shipley, G. G. (1987) *Biochemistry 26*, 623–633.

McDaniel, R. V., McIntosh, T. J., & Simon, S. A. (1983) *Biochim. Biophys. Acta 731*, 97–108.

McIntosh, T. J., & Simon, S. A. (1986) *Biochemistry 25*, 4058–4066.

McIntosh, T. J., McDaniel, R. V., & Simon, S. A. (1983) *Biochim. Biophys. Acta 731*, 109–114.

Moody, M. F. (1963) *Science (Washington, D.C.) 142*, 1173–1174.

Nagle, J. F., & Wilkinson, D. A. (1978) *Biophys. J. 23*, 159–175.

Paltauf, F., Hauser, H., & Phillips, M. C. (1971) *Biochim. Biophys. Acta 249*, 539–547.

Ranck, J. L., Keira, T., & Luzzati, V. (1977) *Biochim. Biophys. Acta 488*, 432–441.

Ruocco, M. J., & Shipley, G. G. (1982a) *Biochim. Biophys. Acta 684*, 59–66.

Ruocco, M. J., & Shipley, G. G. (1982b) *Biochim. Biophys. Acta 691*, 309–320.

Ruocco, M. J., Siminovitch, D. J., & Griffin, R. G. (1985a) *Biochemistry 24*, 2406–2411.

Ruocco, M. J., Makriyannis, A., Siminovitch, D. J., & Griffin, R. G. (1985b) *Biochemistry 24*, 4844–4851.

Sayre, D. (1952) *Acta Crystallogr. 5*, 843.

Seddon, J. M., Cevc, G., & Marsh, D. (1983) *Biochemistry 22*, 1280–1289.

Serrallach, E. N., Dijkman, R., de Haas, G. H., & Shipley, G. G. (1983) *J. Mol. Biol. 170*, 155–174.

Shannon, C. E. (1949) *Proc. Inst. Radio Eng. N.Y. 37*, 10–21.

Siminovitch, D. J., Jeffrey, K. R., & Eibl, H. (1983) *Biochim. Biophys. Acta 727*, 122–134.

Simon, S. A., & McIntosh, T. J. (1984) *Biochim. Biophys. Acta 773*, 169–172.

Snyder, F., Lee, T.-C., & Wykle, R. L. (1985) in *The Enzymes of Biological Membranes* (Martonosi, A., Ed.) Vol. 2, pp 1–58, Plenum Press, New York.

Tardieu, A., Luzzati, V., & Reman, F. C. (1973) *J. Mol. Biol. 75*, 711–733.

Torbet, J., & Wilkins, M. H. F. (1976) *J. Theor. Biol. 62*, 447–458.

Vaughan, D. J., & Keough, K. M. (1974) *FEBS Lett. 47*, 158–161.

Worthington, C. R., & Blaurock, A. E. (1969) *Biophys. J. 9*, 970–990.

Worthington, C. R., King, G. I., & McIntosh, T. J. (1973) *Biophys. J. 13*, 480–494.